

Joint Back Projection and Residual Networks for Efficient Image Super-Resolution

Zhi-Song Liu, Wan-Chi Siu and Yui-Lam Chan

Centre for Signal Processing, Department of Electronic and Information Engineering
The Hong Kong Polytechnic University
Hung Hom, Kowloon, Hong Kong
zhisong.liu@connect.polyu.hk, enwcsi@polyu.edu.hk

Abstract— Benefiting from the great power of graphic processor units, researchers can now come up with more and more sophisticated and complex deep learning structures to solve computer vision problems in various fields with excellent results. However, real-time performance is the bottleneck for deep learning in some applications, like image super-resolution. In this paper, we propose an image super-resolution making use of both the advantages of Back Projection and Residual Networks (BPRN). It generalizes the residual networks as a hierarchical back projection process. We use both convolution and deconvolution to down- and up-sample images to feedback the residues for super-resolution. Furthermore, we come up with a Lighter BPRN (L-BPRN) model to achieve similar state-of-the-art PSNR but fewer network parameters. The testing process is much faster and also accurate for image super-resolution with different scaling factors. Compared with recent deep learning based image super-resolution approaches, experimental results show that our proposed methods can achieve the state-of-the-art PSNR and SSIM performance as well as fast realization.

Keywords—deep learning, image super-resolution, residual networks, back projection

I. INTRODUCTION

Image Super-Resolution (SR) has gained much attention in the past decade. The task of SR is to reconstruct a high-resolution (HR) image from the low-resolution (LR) image with different scales. This ill-posed problem makes the reconstruction process more difficult when we up-sample the LR image with larger scales. The realization of good SR approaches in practical application requires a general model that can handle different up-scaling factors and degrading factors such as blur or noises.

To super-resolve a LR image, traditional learning based approaches tackle the complex image-space reconstruction as a patch based mapping problem. The basic idea is to decompose the image into small patches with simple features so that each patch can be reconstructed by an approximate linear mapping model. To learn a robust mapping model, the patch data need to be classified into groups and each group contains both LR and HR patch pairs to estimate the mapping models. This “divide and conquer” strategy requires external or internal patch pairs to extract the latent relationship between LR and HR images. Different classification methods [2]-[11] have been investigated for image super-resolution, including kNN [3]-[5], sparsity [2]-[3], Gaussian Mixture Model [6]-[7], Random

Forest [8]-[11] and so on. To classify the patch data into different groups, hand crafted features are designed to extract the key information that distinctly maximizes the margin between patch groups.

However, traditional learning based SR approaches suffer from the lack of accuracy and generalization on real-time application because of the linear or sublinear approximation on data reconstruction and limited computation power on big data. The advent of Convolutional Neural Network (CNN) accelerates the development of image super-resolution [14]-[23]. The end-to-end structure minimizes the mean squared error between LR and HR images by varying network design. From shallow auto encoder structure to deep residual networks, the more complexity of the CNN structure, the better performance we can achieve. In order to suit for super-resolution with different upscaling factors, a lot of works combine the LR images with different resolutions and the corresponding HR images to learn the robust feature maps for multiscale super-resolution. To ease the computational complexity, deconvolution [15] and subpixel reconstruction [18] were proposed to up-sample the LR image to the desired resolution and then enhance the edge and texture areas. Most recently, Enhanced Deep Super-Resolution (EDSR) [22] and Deep Back-Projection Networks (DBPN) [23] approaches can achieve two of the best SR results in terms of both PSNR and also visual fidelity by exploring deeper and complex CNN structures. Though CNN based image super-resolution methods improve both quantitative and qualitative performance, the deep complex networks make the reconstruction both difficult for fair analysis or real-time application.

To address these drawbacks, we combine Back Projection and Residual Network (BPRN) for efficient image super-resolution. We propose a multi-stage CNN model with full exploitation of the residual information to learn the nonlinear mapping relationships between LR and HR images. Benefited from back projection [1] mechanism, we expand the iterative residual refinement into a cascaded enhanced network to gradually minimize the residue between LR and HR images. In this paper, we analyze our models on different datasets by comparing peak signal-to-noise ratio (PSNR) and computation time with other state-of-the-art CNN based SR approaches [14]-[23]. Meanwhile, we also give more investigation on the effect of number of convolution layers and filters to find the

optimal CNN structure. In summary, the main contributions of this work are threefold:

- We propose a general image super-resolution model that can super-resolve LR to multiscale resolution.
- We combine Back Projection and Residual Network (BPRN) to super-resolve LR images layer by layer to improve the visual quality.
- Finally, we compare the structure of the BPRN with other CNN models to come up with a lighter CNN model (L-BPRN) to speed up the computation time to achieve similar performance in terms of both subjective and objective qualities.

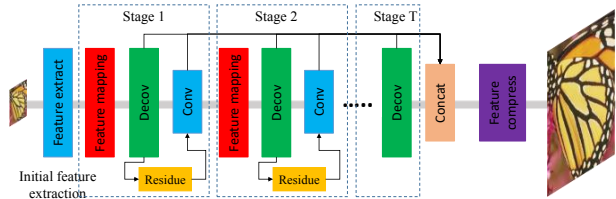


Figure 1. Proposed BPRN model

II. PROPOSED METHOD

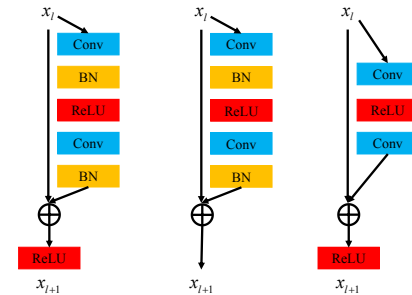
Fig.1 illustrates the complete BPRN network for image super-resolution. It contains three stages of residual enhancement process. Given a LR image with $M \times N$, we directly input it into the model and output a SR image with the desired dimensions $\alpha M \times \alpha N$, where $\alpha > 1$. Each stage minimizes the residual loss between LR and SR feature maps by the mechanism of back projection.

A. Back Projection and Residual Networks

In this part, we introduce the BPRN networks for image super-resolution. Recently, researchers give much investigation on deep learning based image super-resolution methods. Very Deep convolution networks for Super-Resolution (VDSR) [16] makes full use of convolution calculation to design a 20-layer convolutional networks with good super-resolution results. To avoid the vanishing gradient problem, Super-Resolution using ResNet (SRResNet) [21] employs the ResNet structure to perform super-resolution to achieve much better image quality. Furthermore, EDSR modifies the ResNet structure to simplify the residual blocks to boost up the performance of super-resolution. To ease the computation on realization, [15], [19] and [23] give more studies on using deconvolution to up-sample LR images to avoid introducing errors during the initial up-sampling process. Based on back projection, DBPN [23] stacks more deconvolution layers to form a cascaded residual network that can gradually feedback the loss caused by up-sampling to generate deeper features to reconstruct the SR images.

The idea of back projection can be generalized as a hierarchical residual network with error feedback procedure. To further study the relationship between the back projection and residual network, let us compare the fundamental blocks of different networks.

In Fig. 2, we show the residual blocks in ResNet [12], SRResNet [21] and EDSR [22] of their different structures. From ResNet to SRResNet, the ReLU layer is removed after addition process to preserve the negative residual part. Furthermore, it has been experimentally proven that the batch normalization layer is useless for image super-resolution because that the LR and HR images are normalized into range [0,1] as inputs for training. Normalizing features would cause extra information compression which discourages the model to achieve better super-resolution results. Hence, the EDSR model removes Batch Normalization layer to achieve better results.



(a) ResNet (b) SRResNet (c) EDSR

Figure 2. Residual blocks in different SR methods

Back-projection is an efficient iterative process to improve the data fidelity of super-resolution by minimizing the loss between the original LR image and the down-sampled SR image. Assuming we have a LR image with $X \in \mathbf{R}^{m/2 \times n/2}$ and HR image $Y \in \mathbf{R}^{m \times n}$. Let D be down-sampling operation and H be blurring operation.

$$\min \frac{1}{2} \| X - DHY \|^2 \quad (1)$$

Back-projection aims to iteratively update the SR image $Y_0 \in \mathbf{R}^{m \times n}$ by processing inverse up-sampling operation on residual LR images as follows:

$$Y_0(t+1) = Y_0(t) - H^* D^* (DHY_0(t) - X) \quad (2)$$

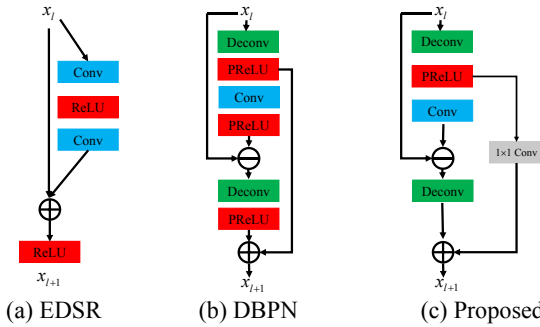
where D^* is the up-sampling operator and H^* is the deblurring operator. In the previous study, we need to assume a certain down-sampling and blurring operators and their inverse operators so that we can perform the iterative updating. Generally, researchers assume Bicubic as the up-/down-sampling operator for super-resolution. There are many deep learning based image super-resolution methods [14]-[17] which up-sample the LR image by *Bicubic* to obtain the initial HR image Y_0 as the input to match the dimension of the ground truth HR image and learn the residual between Y_0 and Y . However, we can employ the deconvolution procedure into residual block structure as a generalization of up-sampling operation in image super-resolution. By combine convolution and deconvolution process, we can generalize the back-projection as a type of residual network as shown below.

In Fig. 3, we compare the residual block in EDSR [22], back projection unit in DBPN [23] and the modified residual

block in our proposed BPRN. Our proposed model removes two PReLU layers to simulate the EDSR model for avoiding unnecessary nonlinear mapping at skip connection, and adds an 1×1 identity layer on the residual part as shown in Eq. (3) to introduce the weighting mapping in order to learn more complex features for reconstruction.

$$x_{l+1} = W_{up}(x_l - W_{down}(W_{up}(x_l))) + W_{weight}(W_{up}(x_l)) \quad (3)$$

In Eq. (3), W_{up} is the deconvolution layer and W_{down} is convolution layer and W_{weight} is the weighting layer. With the extra weighting layer, the shortcut connection between the input and output can be tuned by a weight layer to achieve better reconstruction.



(a) EDSR (b) DBPN (c) Proposed
Figure 3. Compare residual block among the proposed BPRN, EDSR and DBPN

B. Lighter BPRN Networks

Let us further compare the network complexity of BPRN and other SR methods. We come up with a Lighter BPRN model (L-BPRN) which uses fewer parameters to achieve similar performance with much less computation times. The model is shown in Fig. 4.

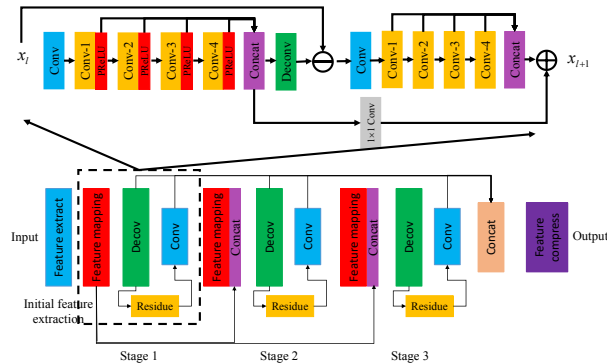


Figure 4. L-BPRN model

We reduce the number of filters and increase the number of layers of convolution filters to learn deeper features for deconvolution. We use a final concatenation layer to combine outputs of all $T (T>1)$ stages together to boost up the final super-resolution result. We summarize the structure parameter in Table I. Note that for L-BPRN, the number of filters in convolution layers is 32 and the number of filters in deconvolution layers is 16.

TABLE I. Number of network parameters of different methods on scaling factor 4×

Options	Model	Stages	Filter size	Filter no.	Parameters
SRResnet	-	-	3×3	64	1.5M
EDSR	-	-	3×3	128	43M
DBPN	S	2	8×8	64	3.2M
	M	4	8×8	64	7.4M
Proposed L-BPRN	L	6	8×8	64	11.6M
	S	2	8×8	32/16	4.0M
Proposed L-BPRN	M	3	8×8	32/16	6.3M
	L	4	8×8	32/16	8.5M

III. EXPERIMENTS

A. Training details and implementation

In the proposed networks, we firstly have two convolution layer of size 3×3. For deconvolution layers, we changed the filter size based on the up-scaling factor. For 4× enlargement, we used 8×8 filter with stride 4 and padding 2. For 8× enlargement, we used 12×12 filter with stride 8 and padding 4. We initialized the weights by [13] and used parametric rectified linear units (PReLU) instead of rectified linear units (ReLU) as the activation layer because PReLU allows small leakage along the negative values.

We trained all networks using image from DIV2K [25] without using augmentation (no rotation or flipping operation). We obtained the LR image by using *Bicubic* in MATLAB and we generated the LR-HR training image pairs by cropping 32×32 regions from LR images and 32α×32α regions from HR images, respectively, where α is the up-sampling factor. The learning rate is 10⁻⁴ for all layers and the total iteration number was 10⁶. For gradient descent optimization, we used Adam with momentum 0.9 and weight decay 10⁻⁴. All experiments were conducted using Caffe with two NVIDIA GTX 1080 Ti GPUs.

B. Model analysis

Let us compare the original BPRN model and L-BPRN model with different number of stages, for which we had conducted multiple networks S(T=2), M(T=3) and L(T=4) similar to DBPN S(T=2), M(T=4) and L(T=6). The results of 4× enlargement on Set5 dataset are shown in Fig. 5.

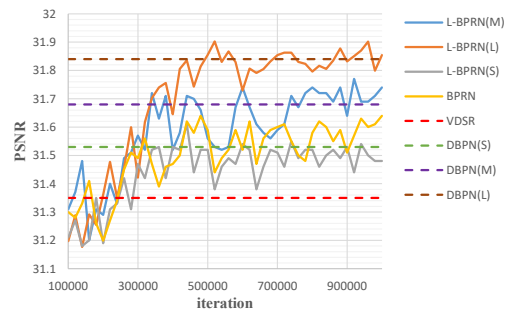


Figure 5. The model analysis on depth evaluation

Our proposed BPRN can outperform the VDSR [16] at least 0.3 dB in PSNR. For BPRN, we used the same structure ($T=2$) as in DBPN(S) but with our proposed residual block, we can see that BPRN can improve over 0.1 dB in PSNR which proves the significance of our proposed residual block model. For L-BPRN, compared with DBPN with different number of stages (S, M, L), our proposed method can achieve higher or similar performance. In L-BPRN ($T=4$), it can achieve similar PSNR compared to the DBPN ($T=6$) but with only 60% parameters of the DBPN.

C. Data-ensemble Enhanced BPRN

To fully make use of the trained BPRN model, we can flip and rotate the LR image to generate eight augmented inputs $\{X, X_r^f\}$ for each image, where $r=0^\circ, 90^\circ, 180^\circ, 270^\circ$ and f is flipping operation, including the original LR image. For each augmented image, we generated its corresponding HR image and then we rotated it back to the original geometry $\{Y_r^T, Y_r^{fT}\}$. Finally, we averaged all the results together to obtain the enhanced BPRN or L-BPRN results (BPRN+ or L-BPRN+).

D. Model-ensemble Enhanced BPRN

Meanwhile, from experimented observation, the performance of the proposed models changes when the number of iterations increases. Hence, we can choose the top K (in our case $K=1$) models with lowest loss (or highest PSNR) and average them together to form the final BPRN models (M-BPRN or M-BPRN-L). This interesting feature is shown in Fig. 6:

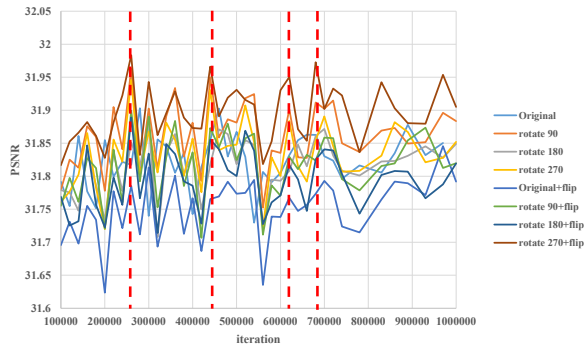


Figure 6. Model-ensemble Enhanced BPRN

In Fig. 6, the BPRN models with top-4 PSNR performance at different augmented version of LR images are marked in red lines. Hence, from 8 augmented images, 4 models with highest PSNR were selected and averaged together to form the final robust model for testing.

E. Comparison with other SR methods

To confirm the performance of our proposed methods, we compare the super-resolution quality and computation complexity with 7 state-of-the-art SR algorithms: A+ [5], CRFSR [10], Super-Resolution via Convolutional Neural Network (SRCNN) [14], VDSR [16], SRResNet [21] and DBPN [23] on dataset Set5 [4], Set14 [4], BSD100 [24] and Urban100 [3] on scaling factors $2\times$ and $4\times$.

PSNR [26] and SSIM [27] are used to evaluate the SR performance. All RGB images were converted to YUV color space and the Y channel was used for evaluation. For SR with a scaling factor of α , we cropped α pixels near image boundary before calculation. Note that each up-scaling factor, we individually train a model for testing. Let us show this complete comparison of SR quality in TABLE II. We can see that our proposed method can achieve the second highest PSNR compared with the state-of-the-art DBPN methods. As for other deep learning based methods or traditional machine learning based methods, our proposed work can outperform them for about 0.2~2 dB in terms of PSNR.

Besides the SR quality comparison, we also measure the computational complexity in terms of computation time to show the tradeoff between SR quality and efficiency. We tested many data set. Let us use the computation time of Set5 dataset on scaling factors $4\times$ by Caffe implementation as a typical example. The methods for comparison includes: Bicubic, A+ [5], CRFSR [10], SRCNN [14], VDSR [16], Deep Recursive Residual Network (DRRN) [20], SRResNet [21] and DBPN [23].

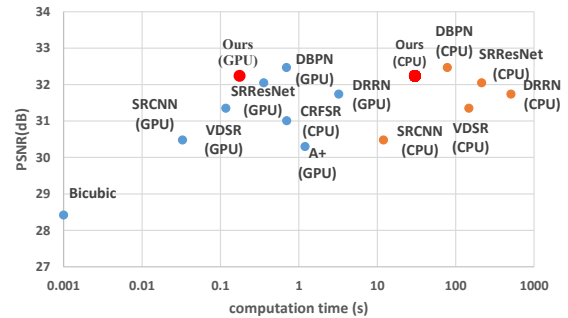


Figure 7. Computation time comparison with other works on $4\times$ super-resolution on Set5 dataset

In Fig. 6, we can see that our proposed L-BPRN methods can achieve the fastest realization while remain very high PSNR performance. In GPU platform, L-BPRN is only slower than VDSR for 0.05 s but achieves 0.9 dB improvement in terms of PSNR. For CPU platform, except for very early work SRCNN, L-BPRN is the fastest deep learning based methods, which costs less than 30% of the computation of other state-of-the-art SR methods. Especially, L-BPRN uses only 0.17 s to achieve 32.24 dB, and the DBPN achieves 32.48 dB but requires 0.69 s computation time. The improvement on computation time of our proposed L-BPRN is very efficient for real time application.

Finally, in order to know more about the qualitative performance, we have shown the visual comparison between different works in Fig. 8 to Fig. 10. In Fig. 8, we can see the eyelash part is clearer using our proposed approach. In Fig. 9, we can see the pattern of the dome is reconstructed well using our proposed approach which other methods can only reconstruct the basic skeleton of the pattern. In Fig. 10, compared with other methods, our proposed approach can reconstruct the stripes on zebras pretty clearly.

TABLE II. PSNR and SSIM comparison between state-of-the-art SR algorithms for scaling factor 2× and 4×

Algorithm	Scale	Set5		Set14		BSD100		Urban100	
		PSNR	SSIM	PSNR	SSIM	PSNR	SSIM	PSNR	SSIM
Bicubic	2	33.65	0.930	30.34	0.870	29.56	0.844	26.88	0.841
A+[5]	2	36.54	0.954	32.40	0.906	31.22	0.887	29.23	0.894
CRFSR[10]	2	37.20	0.955	32.82	0.909	31.79	0.894	30.55	0.910
SRCNN[14]	2	36.65	0.954	32.29	0.903	31.36	0.888	29.52	0.895
VDSR[16]	2	37.53	0.958	32.97	0.913	31.90	0.896	30.77	0.914
DRRN[20]	2	37.74	0.959	33.23	0.913	32.05	0.897	31.23	0.919
SRResNet[21]	2	-	-	-	-	-	-	-	-
DBPN[23]	2	38.09	0.960	33.85	0.919	32.27	0.900	33.02	0.931
L-BPRN	2	37.88	0.959	33.68	0.916	32.15	0.898	32.89	0.925
Bicubic	4	28.42	0.810	26.10	0.704	25.96	0.669	23.15	0.659
A+[5]	4	30.30	0.859	27.43	0.752	26.82	0.710	24.34	0.720
CRFSR[10]	4	31.01	0.870	27.87	0.761	27.05	0.710	24.78	0.721
SRCNN[14]	4	30.49	0.862	27.61	0.754	26.91	0.712	24.53	0.724
VDSR[16]	4	31.35	0.882	28.03	0.770	27.29	0.726	25.18	0.753
DRRN[20]	4	31.68	0.888	28.21	0.772	27.38	0.728	25.44	0.764
SRResNet[21]	4	32.05	0.891	28.53	0.780	27.57	0.735	26.07	0.784
DBPN[23]	4	32.47	0.898	28.82	0.786	27.72	0.740	27.08	0.795
L-BPRN	4	32.24	0.894	28.61	0.782	27.62	0.737	26.89	0.791

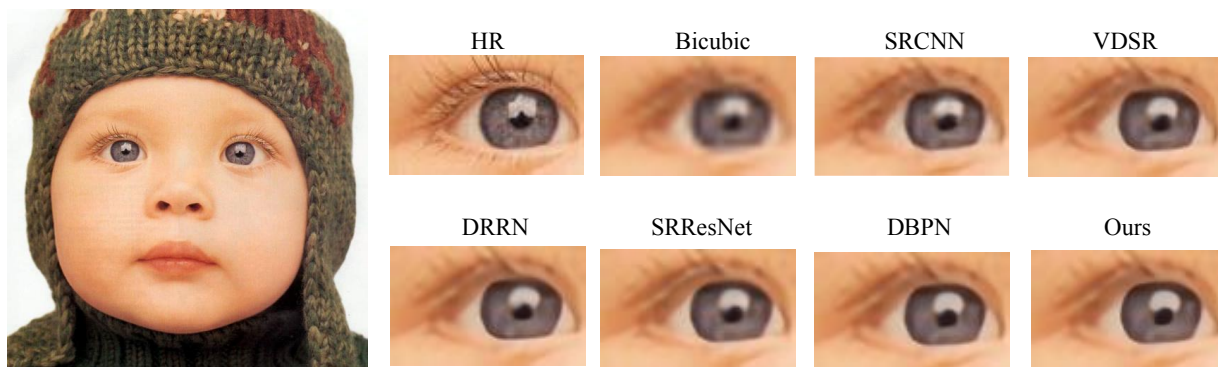


Figure 8. Visual quality comparison of our model with other works on 4× super-resolution on baby.bmp in Set5

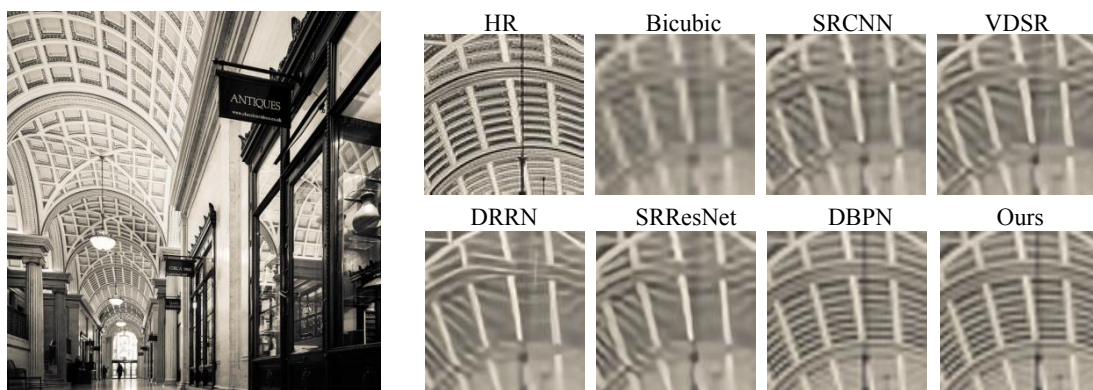


Figure 9. Visual quality comparison of our model with other works on 4× super-resolution on img_083.bmp in Urban100

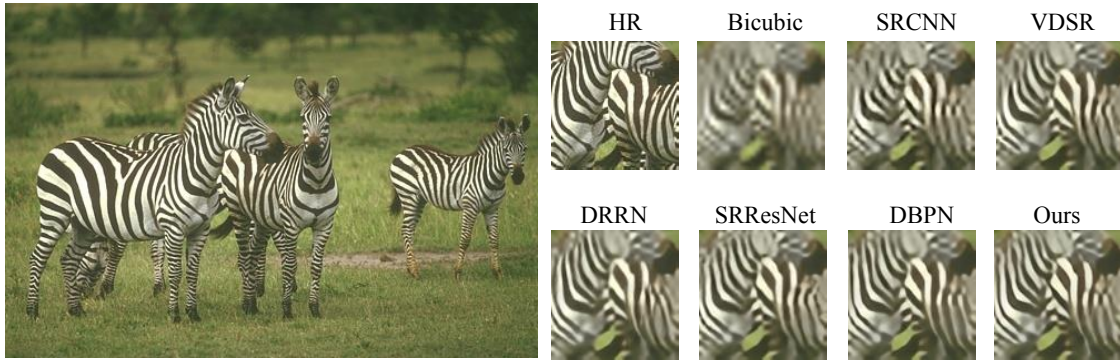


Figure 10. Visual quality comparison of our model with other works on 4x super-resolution on zebra.bmp in BSD100

IV. CONCLUSIONS

In this paper, we propose an image super-resolution using Back Projection and Residual Network (BPRN) and Lighter BPRN (L-BPRN) deep learning based models to achieve state-of-the-art performance in terms of image quality and also fast computation. We have investigated the ResNet and back projection procedure and proposed a generalized residual network for image super-resolution by introducing the back projection mechanism. Not only we come up with the proposed residual networks, we have also proposed to use fewer parameters to train the L-BPRN network that can efficiently realize image super-resolution in real-time to ease the computation. A large number of experiments on different datasets and scaling factors indicate that the proposed methods can outperform other state-of-the-art deep learning based methods. In the future, we will consider a modification on convolution layers of the proposed works on video super-resolution to achieve faster realization for applications.

ACKNOWLEDGMENT

This work was supported by the Centre for Signal Processing, Department of Electronic and Information Engineering, The Hong Kong Polytechnic University (1-BBA2 and G-YBKG), and a grant from the Research Grants Council of the Hong Kong Special Administrative Region, China (Grant No. PolyU 5243/13E).

REFERENCES

[1] M. Irani and S. Peleg, "Improving resolution by image registration," CVGIP: Graphical models and image processing, 53(3):231-239, 1991.
 [2] J. Yang, J. Wright, T. Huang, and Y. Ma, "Image superresolution via sparse representation," *IEEE Trans. on Image Process*, vol. 19, no. 11, 2010.
 [3] J.-B. Huang, A. Singh, and N. Ahuja, "Single image superresolution from transformed self-exemplars," Proceedings, pp. 5197-5206., IEEE International Conference on Computer Vision and Pattern Recognition (CVPR'2015), 2015, Boston, MA.
 [4] R. Timofte, V. De Smet, L. Van Gool, "Anchored neighborhood regression for fast example-based super-resolution," Proceedings, pp. 1920-1927., IEEE International Conference on Computer Vision (ICCV'2013), 2013, Sydney, Australia.
 [5] R. Timofte, V. De Smet, and L. Van Gool. "A+: Adjusted anchored neighborhood regression for fast super-resolution," Proceedings, pp. 111-126., IEEE International Conference on Asian Conference on Computer Vision (ACCV'2014), 2014, Singapore.

[6] L. Sun, S. Cho, J. Wang, and J. Hays. "Good Image Priors for Non-blind Deconvolution - Generic vs. Specific," Proceedings, pp. 231-246., IEEE International Conference on European Conference on Computer Vision (ECCV'2014), 2014, Zurich.
 [7] H. He and W. C. Siu, "Single image super-resolution using Gaussian process regression," Proceedings, pp. 449-456., IEEE International Conference on Computer Vision and Pattern Recognition (CVPR'2011), 2011, Colorado Springs.
 [8] Zhi-Song Liu, Wan-Chi Siu and Jun-Jie Huang, "Image super-resolution via weighted random forest," Proceedings, pp. 1019-1023., IEEE International Conference on Industrial Technology (ICIT'2017), 2017, Toronto, ON.
 [9] Zhi-Song Liu, Wan-Chi Siu and Yui-Lam Chan, "Fast image super-resolution via Randomized Multi-split Forests," Proceedings, pp. 1-4., IEEE International Conference on Symposium on Circuits and Systems (ISCAS'2017), 2017, Baltimore, MD.
 [10] Zhi-Song Liu and Wan-Chi Siu, "Cascaded random forests for fast image super-resolution," accepted by IEEE International Conference on Image Processing (ICIP'2018), Greece, 2018.
 [11] Jun-Jie Huang and Wan-Chi Siu, "Learning Hierarchical Decision Trees for Single Image Super-resolution," *IEEE Trans. Circuits and Systems for Video Technology*, vol. PP, no. 99, Dec. 2015.
 [12] K. He, X. Zhang, S. Ren, and J. Sun, "Delving deep into rectifiers: Surpassing human-level performance on imagenet classification," Proceedings, pp. 1026-1034, IEEE International Conference on Computer Vision (ICCV'2015), 2015, Santiago, Chile.
 [13] K. He, X. Zhang, S. Ren, and J. Sun, "Deep residual learning for image recognition," Proceedings, pp. 770-778., IEEE International Conference on Computer Vision and Pattern Recognition (CVPR'2016), 2016, Las Vegas, Nevada.
 [14] C. Dong, C. C. Loy, and X. Tang, "Image super-resolution using deep convolutional networks," *IEEE Trans. Pattern Analysis and Machine Intelligence*, vol. 38, No. 2, Feb, 2016.
 [15] C. Dong, C. C. Loy, and X. Tang, "Accelerating the super-resolution convolutional neural network," Proceedings, pp. 391-407., IEEE International Conference on European Conference on Computer Vision (ECCV'2016), 2016, Amsterdam, the Netherlands.
 [16] J. Kim, J. KwonLee, and K. MuLee, "Accurate image super-resolution using very deep convolutional networks," Proceedings, pp. 1646-1654., IEEE International Conference on Computer Vision and Pattern Recognition (CVPR'2016), 2016, Las Vegas, Nevada.
 [17] J. Kim, J. Kwon Lee, and K. Mu Lee, "Deeply-recursive convolutional network for image super-resolution," Proceedings, pp. 1637-1645., IEEE International Conference on Computer Vision and Pattern Recognition (CVPR'2016), 2016, Las Vegas, Nevada.
 [18] W. Shi, J. Caballero, F. Huszar, J. Totz, A. P. Aitken, R. Bishop, D. Rueckert, and Z. Wang, "Real-Time Single Image and Video Super-Resolution Using an Efficient Sub-Pixel Convolutional Neural Network," Proceedings, pp. 1874-1883., IEEE International Conference

- on Computer Vision and Pattern Recognition (CVPR'2016), 2016, Las Vegas, Nevada.
- [19] W.-S. Lai, J.-B. Huang, N. Ahuja, and M.-H. Yang, "Deep laplacian pyramid networks for fast and accurate super-resolution," Proceedings, IEEE International Conference on Computer Vision and Pattern Recognition (CVPR'2017), 2017, Honolulu, Hawaii.
- [20] Y. Tai, J. Yang, and X. Liu, "Image super-resolution via deep recursive residual network," Proceedings, IEEE International Conference on Computer Vision and Pattern Recognition (CVPR'2017), 2017, Honolulu, Hawaii.
- [21] C. Ledig, L. Theis, F. Husz'ar, J. Caballero, A. Cunningham, A. Acosta, A. Aitken, A. Tejani, J. Totz, Z. Wang, et al, "Photo-realistic single image super-resolution using a generative adversarial network," Proceedings, IEEE International Conference on Computer Vision and Pattern Recognition (CVPR'2017), 2017, Honolulu, Hawaii.
- [22] B. Lim, S. Son, H. Kim, S. Nah, and K. M. Lee, "Enhanced deep residual networks for single image super-resolution," Proceedings, IEEE International Conference on Computer Vision and Pattern Recognition Workshop (CVPRW'2017), 2017, Honolulu, Hawaii.
- [23] M. Haris, G. Shakhnarovich, and N. Ukita, "Deep backprojection networks for super-resolution," Proceedings, IEEE International Conference on Computer Vision and Pattern Recognition (CVPR'2018), 2018, Salt Lake City, Utah.
- [24] P. Arbelaez, M. Maire, C. Fowlkes, and J. Malik, "Contour detection and hierarchical image segmentation," *IEEE Trans. Pattern Analysis and Machine Intelligence*, 33(5):898–916, 2011.
- [25] R. Timofte, E. Agustsson, L. Van Gool, M.-H. Yang, L. Zhang, B. Lim, S. Son, H. Kim, S. Nah, K. M. Lee, et al, "Ntire 2017 challenge on single image super-resolution: Methods and results," Proceedings, pp. 1110–1121., IEEE International Conference on Computer Vision and Pattern Recognition Workshop (CVPRW'2017), 2017, Honolulu, Hawaii.
- [26] M. Irani and S. Peleg, "Motion analysis for image enhancement: Resolution, occlusion, and transparency," *Journal of Visual Communication and Image Representation*, 4(4):324–335, 1993.
- [27] Z. Wang, A. C. Bovik, H. R. Sheikh, and E. P. Simoncelli, "Image quality assessment: from error visibility to structural similarity," *IEEE Trans. on Image Process*, 13(4):600–612, 2004.